Available online at www.sciencedirect.com
ScienceDirect
Catalysis Today 120 (2007) 63–70
CATALYSIS TODAY
www.elsevier.com/locate/cattod

Pd-Zn/Cu-Zn-Al catalysts prepared for methanol oxidation reforming in microchannel reactors

Guangwen Chen *, Shulian Li, Quan Yuan

Dalian Institute of Chemical Physics, Chinese Academy of Sciences, 457 Zhongshan Road, Dalian 116023, China

Available online 14 August 2006

Abstract

Methanol oxidation reforming is an important reaction in the process of hydrogen generation for PEMFC. In this paper, we report the wall coated catalysts in a microchannel reactor for methanol oxidation reforming. The preparation method of the wall coating catalyst was studied in detail, i.e., the sol–gel and solution-coating techniques. To prepare the catalysts for methanol oxidation reforming, the washing-coating layer of CuZnAl was prepared by the sol–gel technique, and then the active layer was coated on it by solution-coating technique with emulsion colloid containing Pd–ZnO particles. Both the supporting layer and catalyst on the stainless steel foils were characterized by scanning electron microscopy (SEM) and X-ray diffraction (XRD). The formed wash-coating layer with ordered arrays of petaloid microcrystallites in layer surface and Pd–Zn alloy crystal phase can be clearly observed. The reaction experimental results indicated that the catalyst prepared have high activity and relatively high stability.

Keywords: Microchannel; Microstructured reactor; Wall coating; Oxidation reforming; Microreactor

1. Introduction

Automotive exhaust is currently one of the major pollution sources. As a pollution-free and energy-saving power supply for electric vehicles, the fuel cell is the best candidate with its high energy conversion efficiency (50–70%) and zero or nearly zero emission. Hydrogen is the fuel for proton exchange membrane fuel cell (PEMFC). The on-board generation of hydrogen from methanol was known as the one of most practical ways for proton exchange membrane (PEM) fuel cells vehicle [1]. However, the miniaturization of hydrogen source is the prerequisite for its practical application [2,3].

Technology for converting methanol into a hydrogen-rich supply for the fuel cells is mainly based on steam reforming, partial oxidation or a combination of both, namely oxidation steam reforming or oxidation reforming or autothermal reforming, in which the methanol oxidation reforming is the most promising way due to its energy saving, fast start-up and quick response of the whole system. Due to thermodynamic constrains of methanol reforming, significant amount of CO as a poisoning impurity of platinum electro-catalyst is produced. It is also necessary to reduce the level of CO in the hydrogen-rich gas to less than 50 ppm, although high CO-resistant electro-catalysts were developed, so the process of preferential oxidation of CO is required.

Great achievements have been reported in the new area of microreactor technology [4,5], it is now attainable to use microchannel reactors in the field of on-board PEMFC hydrogen source via methanol conversion [6]. The small dimension of microchannel geometry is favoring isothermal operating conditions due to high surface-to-volume ratio, enhanced heat and mass transfer and intrinsic safety. The application of microreaction technology can greatly improve the efficiency of systems and diminish their volumes and weights. The review article [6] has made a deep discussion on the developments in portable hydrogen production using microreactor technology. However, catalyst immobilization into the microchannels is still a challenge which is influenced by a low interaction between metallic plate surfaces and catalyst carriers. [7–9].

Three main ways were applied for catalyst immobilization in microchannel, the one is that the reactors or microchannels themselves were made of active materials [10–13], the two others are wall-coating technique and catalysts packed into channels in the form of powder, small pellets or structured strips

* Corresponding author. Tel.: +86 411 84379031; fax: +86 411 4691570.
E-mail address: gwchen@dicp.ac.cn (G. Chen).

0920-5861/$ – see front matter © 2006 Elsevier B.V. All rights reserved.
doi:10.1016/j.cattod.2006.07.004

[14,15], respectively. The shortcoming of the former is much evident due to its low surface-to-volume ratio and low utilization of noble metal, so it is limited in laboratory, while the pressure drop in the microchannels packed with catalysts is somewhat higher due to their small size. In most practical processes, the surface of microchannels must be modified, i.e., with wash-coating layer as catalyst support. The methods can not only enhance the surface-to-volume, but also improve the utilization of active components. The main wall-coating techniques developed are, e.g., preparation of alumina by a CVD process [16], sol–gel methods [17], anodic oxidation of aluminum inside microchannels [18,19], impregnation [20] or solution coating or dip-coating [21], in situ branching polymerization [8], sputtering [22] and hydrothermal synthesis of zeolites [23,24].

The goal of our study was to immobilize the catalyst of Pd-Zn/Cu-Zn-Al for methanol oxidation reforming on the wall of the stainless steel channels. In this paper, we report the methods to immobilize the catalyst in microchannel and to show potential miniaturization of microreactor used in the hydrogen generation system via methanol oxidative reforming. The catalysts were prepared by sol–gel method for wash-coating layer with Cu-Zn-Al and solution-coating method for active layer with emulsion colloid of Pd–Zn particles.

2. Experimental

2.1. Microreactor design

Fig. 1 shows a stainless steel chip of the microreactor made by a chemical etching method. Forty-eight microchannels per chip were separated by 500 μm fins; its width, depth and length were 500 μm, 170 μm and 30 mm, respectively. The entrance and exit areas are triangular shaped with inlets and outlets on opposite sides of the channels array. Volume of microreactor made of four chips was 0.75 ml including microchannels, entrance and exit sections. Prior to prepare catalyst, the metal substrates were cleaned by Na_2SiO_3 solution with the concentration of 30–50 g/l used as emulsifier to remove any oily substances at the temperature of 75 °C and under agitation, then were rinsed with distilled water at the temperature of 60 °C, and cleaned by acetone and de-ionized water, successively. Finally, metal substrates were dried at 110 °C for 2 h [25].

The stainless steel chips with dry and calcined catalyst deposited in the microchannel were assembled into micro-reactor with high heat-resistant inorganic glue and screw-fastening with bolts to assure hermeticity. The exterior structure of microchannel reactor was shown in Fig. 2 [26]. The microreactor consists of four stacked plates and a plate in the middle of them, which is used to control and measure the reaction temperature. The reactant mixture enters through an inlet tube, then flows through the parallel channels and collected in an outlet device. The inlets and outlets of the microreactor are placed on opposite sides of the stack of plates.

2.2. Experimental set-up

The methanol oxidation reforming was carried out in a microchannel reactor at atmospheric pressure. The micro-channel reactor used in this work and the schematic diagram of the testing system were shown in Fig. 3. Prior to the reaction, the catalyst was reduced in situ in a stream of 10% H_2 in N_2 (50 ml/min) at 400 °C for 2 h. The molar ratio of H_2O and O_2 to MeOH in the feed was 1.2 and 0.3, respectively. The mixture of methanol and water was pumped into a vaporizer kept at 200 °C by a micro liquid pump and conveyed into the reactor by air used for carrier gas and oxidant, while N_2 in air as internal standard for product analysis. The air flow was adjusted precisely by a mass flow controller. The reaction temperature in microreactor was controlled at the range of 450–600 °C, gas hourly space velocity (GHSV) was kept at 20,000–180,000 h^{-1}.

2.3. Gas analysis and calculation

The effluent of the reactor was consisted of H_2, CO_2, CO, CH_4 and N_2 as well as H_2O and/or methanol, while CH_4 in effluent is negligible during the experiments. After reaction, the product gases were passed through a cold trap (mixture of ice and water) and a dryer to remove water and methanol, while the dry gas entered an on-line gas chromatograph (GC, 4000A, Beijing East & West Analytical Instruments Inc.) equipped

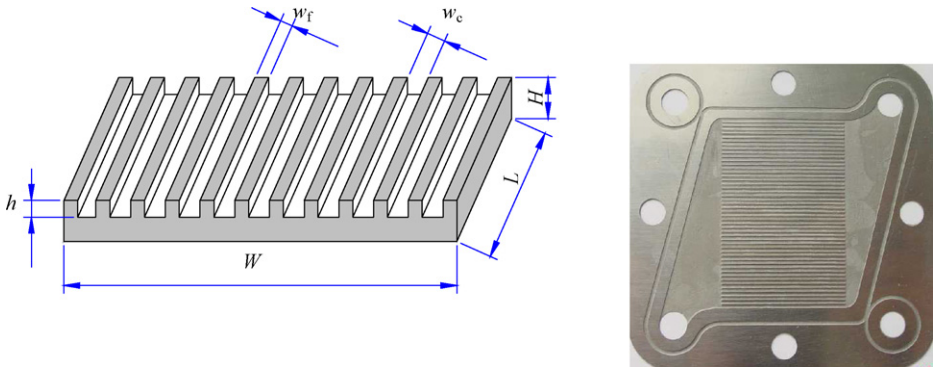

Fig. 1. Chip of microchannel reactor. *W*, width of total channels; w_c, width of single channel; w_f, width of fin; *h*, depth of channel; *H*, thickness of chip; *L*, length of channel.

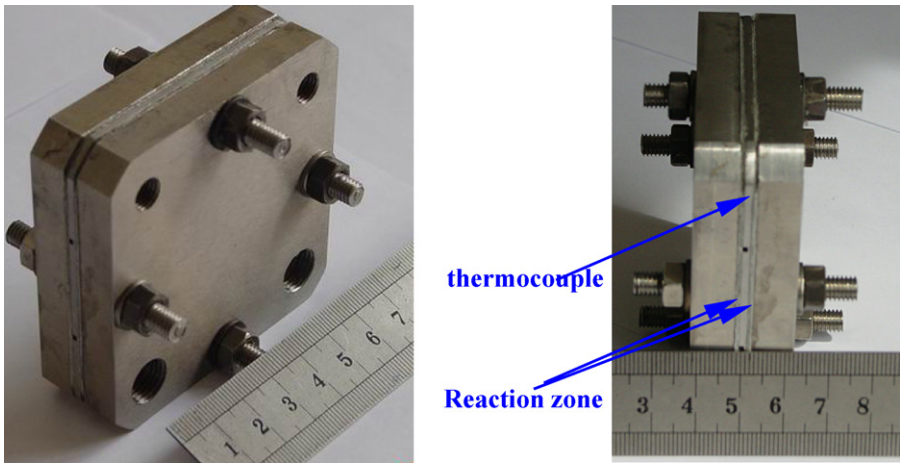

Fig. 2. Photographs of microchannel reactor.

with TCD and FID detectors for analyzing the composition. Detection limit of CO, CO_2 and CH_4 is about 1.0 ppm using a carbon molecular sieve column with carrier gas Ar and FID detector at oven temperature of 100 °C, while O_2 and N_2 were separated using 5 A zeolite with carrier gas H_2 and TCD detector at oven temperature of 70 °C [27].

In this paper, gas hourly space velocity (GHSV) is defined as the ratio of feed volumetric flow rate of methanol to the total effective volume (0.75 ml) of microchannel reactor. Methanol conversion and product yields are calculated based on the flow rate and compositions of the dry gaseous products based on carbon balance and the ratio CO/(CO + CO_2) in the product is referred to CO selectivity. In more detail, the methanol conversion (X_{MeOH}) and CO and CO_2 selectivities (S_{CO} and S_{CO_2}) can be written as following,

$$X_{MeOH} = \frac{F(y_{CO} + y_{CO_2} + y_{CH_4})}{22.4 \times n^0_{MeOH}} \times 100\% \quad (1)$$

$$S_{CO} = \frac{y_{CO}}{y_{CO} + y_{CO_2}} \times 100\% \quad (2)$$

$$S_{CO_2} = \frac{y_{CO_2}}{y_{CO} + y_{CO_2}} \times 100\% \quad (3)$$

where F is referred to the normal volumetric flow of dry reformate gas, ml(STP)/min; n^0_{MeOH} is defined as the molar flow rate of methanol in feed, mmol/min; y_{CO}, y_{CO_2} and y_{CH_4} are defined as the molar compositions of CO, CO_2 and CH_4 in dry reformate gas, respectively.

In order to eliminate the errors caused by catalyst deactivation, all the data were collected when the catalytic activity was kept stable, and the data for each reaction condition was done by 2 or 3 times. Material balances on N_2 were calculated to verify measurement accuracy. In this work, the relative error of N_2 flow rate in feed and dry effluent is less than 3%.

2.4. Catalyst preparation

2.4.1. Wash-coating layer

Pd-Zn/Cu-Zn-Al catalysts in microchannels for methanol oxidation reforming were made up of two layers, i.e., the wash-coating layer of Cu-Zn-Al and active layer of Pd-Zn. The wash-coating layer of Cu-Zn-Al was prepared via sol–gel method. With ethanol as solvent, $Cu(NO_3)_2{\cdot}6H_2O$, $Zn(NO_3)_2{\cdot}6H_2O$ and $Al(NO_3)_3{\cdot}9H_2O$ with molar ratio of 3:6:1 and concentration of 1.0 mol/l were dispersed with a magnetic stirrer for 12 h at

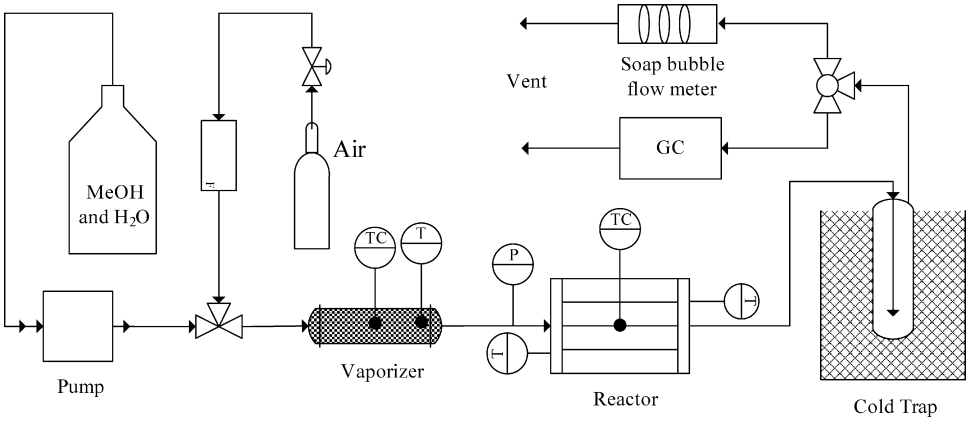

Fig. 3. Schematic diagram of the testing system.

1000 rpm, during continuous stirring, HNO_3 was added to keep the pH at 3–4. The transparent sol of Cu-Zn-Al was formed via the completion of hydrolysis, alcoholization and condensation polymerization. The sol of Cu-Zn-Al was coated onto the microchannel plate using soft fine brush. After drying at room temperature for 1 h and the temperature of 60 °C for 6 h, the plates were calcined in air at 500 °C for 2 h. Repeat above coating, drying and calcining processes, the loading was ca. 20 mg per chip. All the heating up ramps during catalyst preparation were 2 °C/min in this work.

2.4.2. Active layer

The procedure to prepare the active layer of Pd-Zn had three steps. Firstly, ZnO particle was prepared via precipitation method. $H_2C_2O_4$ aqueous solution with 1.8 mol/l was added dropwise into a three-necked round-bottomed flask containing $Zn(NO_3)_2$ aqueous solution with 6 mol/l. The resulting precipitate was filtered and washed with distilled water until neutrality condition. After washing, the precipitate was dried at refrigerator. The dried samples were calcined at 400 °C for 6 h to make them decompose into the ZnO particles with average size of 5–20 μm. Secondly, Pd-Zn powder was prepared by incipient wetness impregnation of ZnO particles with 0.1 g/ml $PdCl_3$ aqueous solution. The particles were dried at room temperature and calcined at 450 °C for 4 h to make them into Pd-Zn powders with the weight ratio of Pd/Zn at 1:20. At last, the emulsion colloids of Pd-Zn were prepared from mixtures of Pd-Zn powder and ZnO particles aqueous suspension milled by ball crusher with 200 rpm for 10 h, HNO_3 was added to adjust the pH between 4 and 5, in which the weight ratio of Pd-Zn powder to ZnO particles was kept at 1:2.8. Then microchannels with Cu-Zn-Al wash-coating layer were coated with Pd-Zn emulsion colloids. Pd-Zn/Cu-Zn-Al catalyst was formed after drying at room temperature and calcining at 450 °C for 6 h. The thickness of active layer is ca. 10 μm calculated, the loading was about 50 mg per chip, while the Pd loading was ca. 2 mg per chip.

2.4.3. Samples for catalyst characterization

A part of the sol of Cu-Zn-Al and emulsion colloids of Pd-Zn were dried and calcinated separately under the same conditions as the plates mentioned above in order to obtain Cu-Zn-Al and Pd-Zn powders with properties as similar as possible to those of the corresponding coatings. These powders were used for XRD, SEM and BET measurements. The specific surface areas of 79.5 m^2/g for Cu-Zn-Al powder and 63.8 m/g for Pd-Zn powder were determined by the BET method using a Auto Chem 2910 (Chemisorber) instrument.

2.4.4. Reduction condition

Prior to catalyst characterization and activity test, all the catalysts in the form of microchannel and powder were reduced with 10% H_2 in N_2 at the flow rate of 50 ml/min at 400 °C for 2 h.

2.4.5. Catalyst characterization

Both the wash-coating layer and active layer of catalysts in microchannel and powders were examined by X-ray diffraction (XRD) for phase identification and to determine the crystallinity on an X'pert PRO diffractometer ((PANalytical Inc.) equipped with Cu Kα radiation with an accelerating voltage of 40 kV and current of 40 mA. The patterns were recorded over the 2θ angle ranging from 20° to 70° at a scan rate of 4°/min.

Scanning electron microscopy (SEM, KYKY-AMRAY 1000B, KYKY Technology Development LTD., China) with work voltage of 25 kV was used for detailed examination of microstructure and morphology of wash-coating layer and catalyst. Prior to the measurements, the samples in microchannel were sputtered with Au. The samples for XRD and SEM are of sliced sheets cut from microchannel chips.

3. Results and discussion

3.1. Cu-Zn-Al coating

3.1.1. SEM morphology

Sol–gel method is one of the most important ways to prepare the thin film of coating layer for Pd membrane, ultrafine metal oxide particles or metal oxide catalyst [17,28,29], and γ-Al_2O_3 was widely used as the coating layer for monolithic catalyst including microchannels. In this work, Cu-Zn-Al was used to prepare the coating layer, for both reasons that metal oxide of Cu-Zn-Al has specific surface area as high as γ-Al_2O_3 and Cu-Zn-Al can be used as catalyst for methanol steam reforming and oxidation reforming as well [17,30]. Cu-Zn-Al sol was prepared via hydrolysis and condensation polymerization of precursor of nitrate mixtures with the aid of acid. The process was strongly dependent on the extent of hydrolysis and solution acidity. When acidity was strong, the rate of hydrolysis and condensation polymerization was high, so the sol will be formed quickly. Experimental results showed that it was in favor of formation of Cu-Zn-Al sol as pH was kept at the range of 3–4. It was still in transparent state after 4 months as pH was lower than 3. Contrarily, precipitation would occur due to hydrolysis of nitrate catalyzed by hydroxyl OH^- when pH is high nearing to alkalinity. Stable sol would be obtained when weight ratio of $CuZnAl:H_2O:HNO_3$ was controlled at ratio of 1:1.9:2.2. The gel layer was formed on stainless steel microchannel plate coated with Cu-Zn-Al sol, and the wash-coating layer was formed after drying and calcining. The morphologies of Cu-Zn-Al wash-coating layer reduced were shown in Fig. 4. From Fig. 4(a) by SEM (top view) with magnification of 20 and Fig. 4(b) with large magnification of 1500, wash-coating layer with ordered arrays of petaloid microcrystallites in layer surface can be clearly observed, showing that wash-coating layer of Cu-Zn-Al is homogeneous, dense.

3.1.2. X-ray diffraction

Fig. 5 shows the XRD patterns of the samples of wash-coating layer Cu-Zn-Al (sol–gel) and Pd-Zn/Cu-Zn-Al catalyst in microchannel reduced at 400 °C for 2 h. From Fig. 5(1), we can see that the weak peaks at Bragg angles 2θ of 42.68° and 50.10° can be attributed to Cu°, for the characteristic peaks of Cu° are at 2θ of 43.47° and 50.67°, while the characteristic

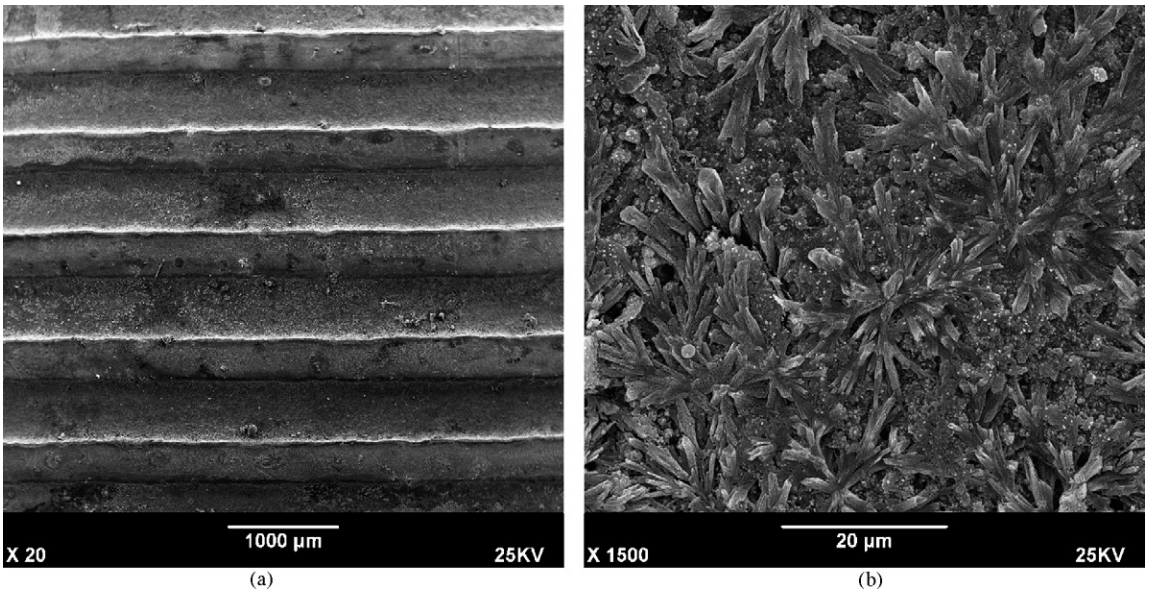

(a) (b)

Fig. 4. SEM image (top view) of CuZnAl wash-coating layer by sol–gel in microchannel wall after reduction at 400 °C for 2 h. Magnification: (a) 20 and (b) 1500.

peaks of stainless steel are at 2θ of 43.70° and 50.80°. In order to discriminate and determine the attribution of these characterization peaks, the Cu-Zn-Al powder was prepared using the same precursor as in microchannel for XRD analysis. From the XRD pattern in Fig. 5(3), the strong peaks at 2θ of 43.10° and 50.19° can be attributed to Cu°, showing that it is rational to ascribe the weak peaks at 2θ of 42.68° and 50.10° to Cu°. Diffraction peaks of Al_2O_3 cannot be detected by XRD in the samples, showing that spinel crystal of $ZnAl_2O_4$ was formed during the calcining process from ZnO and Al_2O_3, partly reason can be ascribed to that crystal radius of Al_2O_3 of 0.51 nm is less than that of ZnO of 0.74 nm, so displacement of ZnO diffraction peaks can be clearly observed. Actually, from the SEM image with magnification of 1500, it can be obviously seen that some fine particles (small white dot) dispersed around the microcrystalline of $ZnAl_2O_4$. We speculated that the fine particles may be Cu°, for the reasons of that ZnO and Al_2O_3 cannot be reduced at the reduction condition (400 °C and 8% H_2 in N_2), and there were no diffraction peaks of elementary substances of Zn and Al, while the diffraction peak of Cu° can be observed in XRD patterns.

3.2. Pd-Zn/Cu-Zn-Al coating

The SEM image (top view, with magnification of 60 and 1500) of Pd-Zn/Cu-Zn-Al catalyst reduced was shown in Fig. 6, it is clear that both Pd-Zn and ZnO particles was in uniform distribution with the dimension of ca 1 μm. The XRD pattern of the same sample was shown in Fig. 5(2). Diffraction peak at Bragg angles 2θ of 41.34° and 43.66° attributed to Pd–Zn alloy crystal phase can be observed in Fig. 5(2), and the diffraction peaks of single Pd crystal phase were not observed, which is consistent with the reports by Chin et al. [31], Liu et al. [32] and Cubeiro and Fierro [33], indicating that Pd–Zn alloy was formed during the reduction process. The diffraction peaks at 2θ of 50.84° attributed to Cu°, and only a slight displacement can be seen, while the diffraction peaks at 2θ of 42.66° shown in Fig. 5(1) attributed to Cu° between the two PdZn peaks seems

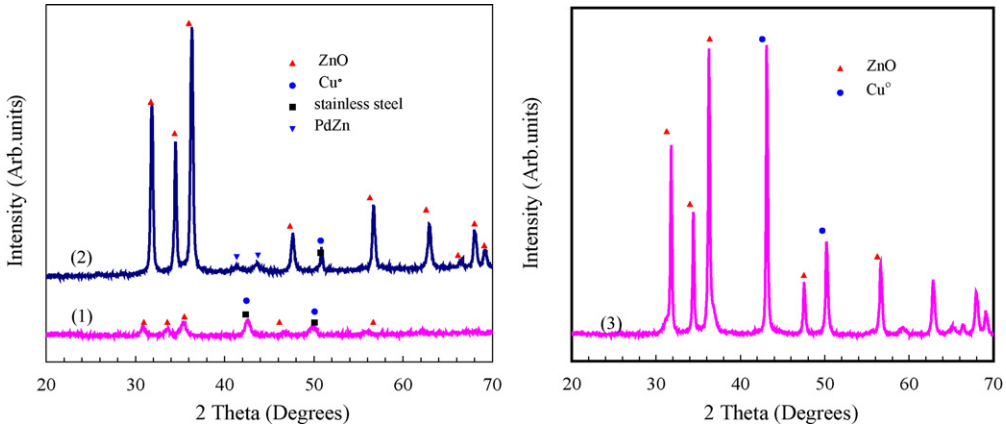

Fig. 5. XRD Patterns of Cu-Zn-Al wash-coating layer, Pd-Zn/Cu-Zn-Al catalyst in stainless steel microchannel plate and Cu-Zn-Al powder after reduction at 400 °C for 2 h: (1) Cu-Zn-Al wash-coating layer, (2) Pd-Zn/Cu-Zn-Al catalyst in microchannel and (3) Cu-Zn-Al powder.

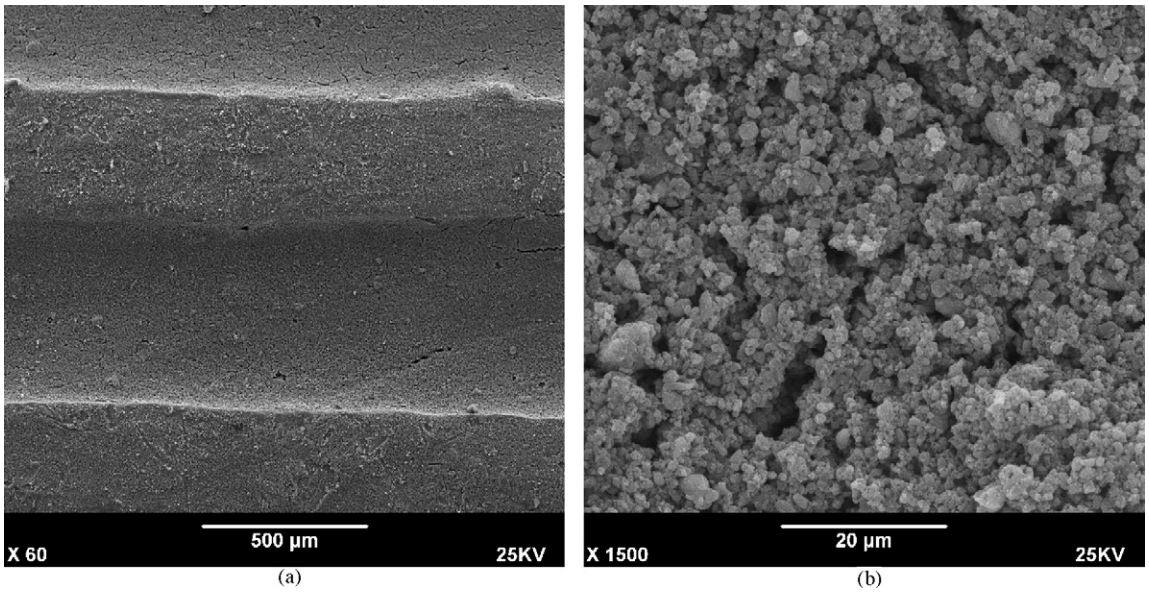

Fig. 6. SEM image (top view) of PdZn/CuZnAl catalysts in microchannels after reduction at 400 °C for 2 h. Magnification: (a) 60 and (b) 1500.

to have restrained and have not appeared in Fig. 5(2). Cu° and Pd–Zn alloy were observed in microchannel catalyst, showing that they would be the catalytic activity centers for methanol oxidation reforming [27,34].

3.3. Adhesion intensity of coating layer

The intensity of adhesion between the coating layer and support is one of the most important factors of the microchannel catalysts. Pieces of both Cu-Zn-Al and Pd-Zn/Cu-Zn-Al in stainless steel microchannels were cut for the tests. The ultrasonic cleaning machine (CQX25-06, Shanghai BRANSON, China) was used to test the adhesive abilities of the coating layers at the output frequency of 25 kHz and output power of 250 W. Table 1 showed the results of the change of the weight fore-and-aft experiment. The weight of the coating layer of Cu-Zn-Al nearly has not any change during the vibration test in the dry state and in water, showing that the strong adhesion between the coating layer and support. The active layer of Pd-Zn/Cu-Zn-Al in microchannel also showed the relative high adhesive intensity with support under the dry state, while it nearly detached from the support during the vibration test immerged in water within 1 min. The results of ultrasonic vibration tests showed that the sol–gel method is feasible to prepare the coating layer in microchannel, whereas the solution-coating technique with emulsion colloid containing particles is not good choice. This indicated that the interaction between the active layer and support was not strong enough to maintain the high activity of catalysis for life test of 1000 h, though the activities of this catalyst was still in a high level during 10 h reaction test.

Table 1
Ultrasonic vibration test of coating layer

Coating layer	Weight of coating layer and substrate (g)		
	Original	After 5 min[a]	1 min[b]
Cu-Zn-Al	1.6571	1.6570	1.6568
Pd-Zn/Cu-Zn-Al	2.6757	2.6757	2.6614

[a] *Note*: vibration under dry state (in air).
[b] Immerged in water.

3.4. Catalyst activity test

The catalytic activity and selectivity for methanol oxidation reforming were plotted in Fig. 7 as a function of gas hourly space velocity in microchannel reactor. The data for catalyst activity were obtained using same catalyst during continuous 10 h test. The methanol conversion in the microchannel reactor was still higher than 91% even at 183,000 h^{-1}, and nearly 100% conversion of methanol can be achieved as GHSV was lower than 137,000 h^{-1}. In microchannel reactor, the reaction rate increased remarkably and conversion was still high even at high GHSV, owing to its high efficient heat and mass transfer with its small dimensions of micron-size. However, grounded on the same reason of its high heat transfer rate (the heat transfer coefficient h in the microreactor can be achieved as high as 1000 W/m^2 K, and it increases with increasing of the flow rate), so that heat in microreactor will be released to the environment quickly, resulting in that microreactor can not be kept at constant reaction temperature without exterior heat input [16]. In Fig. 7, both the control temperature and reaction temperature measured were given, we can see that catalyst bed temperature was nearly identical to controlling temperature and had uniform temperature field in microreactor due to its very high heat transfer.

Fig. 7(b) showed the composition of the dry product gas of methanol oxidation reforming. H_2 has a high value of 50% and CO is lower than 2% under the reaction condition with corresponding CO selectivity lower than 10%. CO is the main poison of the electrode catalyst (Pt) of the PEMFC, so it must be reduced to less than 50 ppm. To attain that, supplementary reactions, such as preferential oxidation, have to be applied.

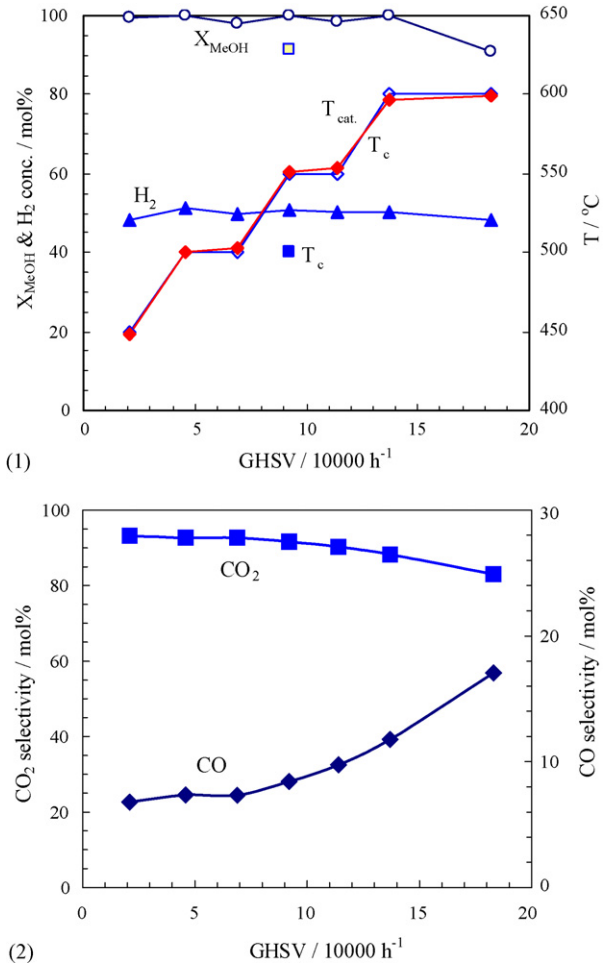

Fig. 7. Catalytic activity on microreactor for production of hydrogen via methanol oxidation reforming O_2/MeOH = 0.30, H_2O/MeOH = 1.2 (molar ratio); In (a) (○,□) methanol conversion; (■,◆) reactor temperature controlled; (◇) catalytic bed temperature; (▲) H_2 concentration in the dry reformate gas; (□) is related to (■) at GHSV = 92,000 h^{-1}.

Considering the possible reaction mechanism in the process of methanol oxidation reforming on Pd-Zn/Cu-Zn-Al catalysts, the following reactions would be included:

$$CH_3OH + 1.5O_2 \rightarrow CO_2 + 2H_2O \text{ (combustion)} \quad (4)$$

$$CH_3OH + 0.5O_2 \rightarrow CO_2 + 2H_2 \text{ (partial oxidation)} \quad (5)$$

$$CH_3OH + H_2O \rightarrow CO_2 + 3H_2 \text{ (steam reforming)} \quad (6)$$

$$CH_3OH \rightarrow CO + 2H_2 \text{ (decomposition)} \quad (7)$$

$$CO + H_2O \leftrightarrow CO_2 + H_2 \text{ (water gas shift)} \quad (8)$$

Unlike Pt/Al_2O_3 catalysts, more than 15% CO (dry gas) was produced in the methanol oxidation reforming, far lower CO concentration was produced by the Pd-Zn/Cu-Zn-Al catalyst than that of calculated from the water gas shift equilibrium. Water gas shift and reverse water gas shift reactions can be negligible in this process. Thus, the decomposition reaction should be responsible for this behavior, especially at high space velocity, shown in Fig. 7(b). From the kinetics view, the activation energy of methanol decomposition is higher than partial oxidation and steam reforming, so higher reaction temperature favors decomposition process, so that more CO would be formed via methanol decomposition under the higher reaction temperature.

In this experiment, we have made a comparative test between the different GHSV (i.e., 21,000, 46,000 and 92,000 h^{-1} respective) under same reaction temperature of 450 °C shown in Fig. 7(1). Methanol conversion of decreased from 99.6 to 91.3% when GHSV increased from 21,000 to 92,000 h^{-1}. This result clearly revealed that the methanol oxidative reforming in microreactor is under the control of kinetic reaction at some conditions, which means the rate of diffusion was higher than intrinsic rate of reaction, especially under higher GHSV. In this paper, one goal was to investigate the maximum extent of miniaturization when microreactor used, the higher GHSV, the higher extent of process intensification. In order to realize the process intensification, so the higher reaction temperature was needed for higher methanol conversion.

As mentioned in Section 1, recent achievements in the microchannel reactors have demonstrated the potential to significantly reduce the transport limitations and hence improving catalyst effectiveness factor. High catalyst effectiveness factor allowed significant reduction in the mass of catalyst used in microchannel reactor while maintaining similar throughput attainable in a conventional reactor. The product gas dry flow was 480 l/h at GHSV of 137,000 h^{-1} (corresponding to contact time of 7.2 ms based on total feed), with 50.2% being hydrogen (240 l/h). The composition was 50.2% hydrogen, 2.0% carbon monoxide, with the rest being nitrogen (from the air feed for reaction) and carbon dioxide. It means that this stainless steel microchannel reactor has the ability to process enough hydrogen for approximately 100 W PEMFC each chip based on 600 l/h hydrogen for 1 kW PEMFC.

4. Conclusions

High active and relatively stable Pd-Zn/Cu-Zn-Al catalysts were successfully incorporated into microchannel plates in order to build an on-board methanol oxidation reformer for hydrogen generation needed for PEM fuel cell. Catalysts developed showed highly activity as indicated by high methanol conversions at high space velocity. Both the Cu-Zn-Al and Pd–Zn alloy particles were distributed uniformly via top view of SEM. The adhesion of coating layer of Cu-Zn-Al with substrate of stainless steel was strong, while the active layer of Pd-Zn exhibited somewhat easy peel off. This implied that the technique of sol–gel for Cu-Zn-Al wash-coating layer was an effective method for preparing catalysts in stainless steel microchannel plates, however way of solution-coating for Pd–Zn particles should be improved further.

Due to the small characteristic dimensions of the microchannel reactor, the effect of heat and mass transport is increased remarkably. The reaction rate increases and the methanol conversion remains high level at very high GHSV. The miniaturization of the hydrogen generation system can be achieved with a microchannel reactor. However, how to improve the system efficiency of microchannel reactor is still

one of the critical problems in order to put it into practical application, especially to improve adhesive of active layer with substrate and reduce the heat loss of microreactor.

Acknowledgements

We gratefully acknowledge the financial supports for this project from National Natural Science Foundation of China and China National Petroleum Corporation (Nos. 20176057, 20122201 and 20490208).

References

[1] R.L. Borup, M.A. Inbody, T.A. Semelsberger, J.I. Tafoya, D.R. Guidry, Catal. Today 99 (2005) 263.
[2] Y. Choi, H.G. Stenger, Appl. Catal. B 38 (2002) 259.
[3] A.Y. Tonkovich, J.L. Zilka, M.J. Lamont, Y. Wang, R.S. Wegeng, Chem. Eng. Sci. 54 (1999) 2947.
[4] K. Jähnisch, V. Hessel, H. Löwe, M. Baerns, Angew. Chem. Int. Ed. 43 (2004) 406.
[5] G. Kolb, V. Hessel, Chem. Eng. J. 98 (2004) 1.
[6] J.D. Holladay, Y. Wang, E. Jones, Chem. Rev. 104 (2004) 4767.
[7] P. Pfeifer, K. Schubert, G. Emig, Appl. Catal. A: Gen. 286 (2005) 175.
[8] J. Kobayashi, Y. Mori, K. Okamoto, R. Akiyama, M. Ueno, T. Kitamori, S. Kobayashi, Science 304 (2004) 1305.
[9] M.T. Janicke, H. Kestenbaum, U. Hagendorf, F. Schüth, M. Fichtner, K. Schuberty, J. Catal. 191 (2000) 282.
[10] C. Horny, L. Kiwi-Minsker, A. Renken, Chem. Eng. J. 101 (2004) 3.
[11] J. Mayer, M. Fichtner, D. Wolf, K. Schubert, in: Proceedings of the third International Conference on Microreaction Technology (IMRET3), Springer, (2000), p. 187.
[12] H. Kestenbaum, O.A. de Lange, W. Schmidt, F. Schuth, W. Ehrfeld, K. Gebauer, H. Löwe, Ind. Eng. Chem. Res. 41 (4) (2002) 710.
[13] V. Hessel, W. Ehrfeld, K. Golbig, C. Hofmann, in: Proceedings of the Third International Conference on Microreaction Technology (IMRET3), Springer, (2000), p. 151.
[14] A. Karim, J. Bravo, A. Datye, Appl. Catal. A: Gen. 282 (2005) 101.
[15] A.L.Y. Tonkovich, S. Perry, Y. Wang, D. Qiu, W.A. Rogers, Chem. Eng. Sci. 59 (2004) 4819.
[16] M. Janicke, H. Kestenbaum, U. Hagendorf, F. Schüth, M. Fichtner, K. Schubert, J. Catal. 191 (2000) 282.
[17] K. Haas-Santo, M. Fichtner, K. Schubert, Appl. Catal. A: Gen. 220 (2001) 79.
[18] G. Wiebmerier, D. Hönicke, J. Micromech. Microeng. 6 (1996) 285.
[19] J.C. Ganley, K.L. Riechmann, E.G. Seebauer, R.I. Masel, J. Catal. 227 (2004) 26.
[20] P. Pfeifer, K. Schubert, M.A. Liauw, G. Emigb, Appl. Catal. A: Gen. 270 (2004) 165.
[21] C.J. Jiang, D.L. Trimm, M.S. Wainwright, N.W. Cant, Appl. Catal. A: Gen. 93 (1993) 245.
[22] A. Kursawe, R. Pilz, H. Dürr, D. Hönicke, in: Proceedings of the Fourth International Conference on Microreaction Technology AIChE Spring Meeting, Atlanta, March 5–9, (2000), p. 227.
[23] E. Rebrov, G. Seijger, H. Calis, M. de Croon, C. Van den Bleek, J. Schouten, Appl. Catal. A: Gen. 206 (2001) 125.
[24] Y.S. Wana, K.L. Yeung, A. Gavriilidis, Appl. Catal. A: Gen. 281 (2005) 285.
[25] G.W. Chen, Q. Yuan, S.L. Li, Chin. J. Catal. 23 (2002) 491.
[26] G.W. Chen, Q. Yuan, H.Q. Li, S.L. Li, Chem. Eng. J. 101 (2004) 101.
[27] S.L. Li, G.W. Chen, F.J. Jiao, H.Q. Li, Chin. J. Catal. 25 (12) (2004) 979.
[28] R.D. Gonzaleza, T. Lopez, R. Gomez, Catal. Today 35 (1997) 293.
[29] P. Vidmar, P. Fornasiero, J. Kašpar, G. Gubitosa, M. Graziani, Catal. Today 77 (2002) 79.
[30] M. Turco, G. Bagnasco, U. Costantino, F. Marmottini, T. Montanari, G. Ramis, G. Busca, J. Catal. 228 (2004) 43.
[31] Y. Chin, R. Dagle, J. Hu, A.C. Dohnalkova, Y. Wang, Catal. Today 77 (2002) 79.
[32] S. Liu, K. Takahashi, M. Ayabe, Catal. Today 87 (2003) 247.
[33] M.L. Cubeiro, J.L.G. Fierro, J. Catal. 179 (1998) 150.
[34] N. Iwasa, S. Masuda, N. Ogawa, N. Takezawa, Appl. Catal. A: Gen. 125 (1995) 145.